Orthogonal Chemical Functionalization of Au/SiO 2 /TiW Patterned Substrates

Jian Zhang, Didier Léonard, Christelle Yeromonahos, Radoslaw Mazurczyk, Thomas Gehin, Stéphane Monfray, Yann Chevolot, Jean-Pierre Cloarec

Orthogonal chemical functionalization of $Au/SiO_2/TiW$ patterned substrates

Jian Zhang[†], Didier Léonard[‡], Christelle Yeromonahos[†], Radoslaw Mazurczyk[†], Thomas Géhin[†], Stéphane Monfray[§], Yann Chevolot[,†] and Jean-Pierre Cloarec[*,†]*

[†]Université de Lyon, Institut des Nanotechnologies de Lyon (INL), UMR CNRS 5270, Ecole Centrale de Lyon, 36 Avenue Guy de Collongue, 69134 Ecully cedex, France

[‡]Univ Lyon, CNRS, Université Claude Bernard Lyon 1, Institut des Sciences Analytiques, UMR 5280, 5, rue de la Doua, F-69100 Villeurbanne, France

[§]STMicroelectronics SA, 850, rue Jean Monnet, 38926, Crolles, France

ABSTRACT

Macropatterned and micropatterned gold/silicon dioxide/titanium tungsten ($Au/SiO_2/TiW$) substrates were orthogonally functionalized: three different molecules (monovalent silane, thiol, and phosphonic acid) were used to specifically form organolayers on Au, SiO_2 or TiW areas of patterned substrates. The orthogonality of the functionalization (i.e., selective grafting of thiol on Au, phosphonic acid on TiW and silane on SiO_2) was assessed by X-ray photoelectron spectroscopy (XPS), time-of-flight secondary ion mass spectrometry (ToF-SIMS), Fourier Transform Infrared Spectroscopy (FTIR) and contact angle measurements. These results are especially promising for the selective anchoring of targets (e.g. biomolecules,

nanoparticles, nanowires, nanotubes or other nano-objects) onto patterned zones of multi-material substrates, such as nanosensors or other nanodevices.

INTRODUCTION

The increasing number of applications of nanotechnology stresses the importance of designing nanoscale features of various chemical, biochemical or physical properties.[1–4] In this perspective, some strategies have been developed to achieve chemical patterns. For example, microcontact printing transfers organic compounds on defined positions of a substrate by stamping.[5,6] Self-assembled monolayers can be patterned by electron or extreme UV irradiation lithography.[7,8] Besides, on multi-material patterned surfaces, one can take advantage of each material chemical reactivity, to achieve site selective chemical functionalization. The so-called orthogonal chemical functionalization was first proposed in 1989.[9] It offers a versatile method for controlling the interfacial properties of each material on patterned substrates. It is based on the combination of top-down fabrication (e.g. optical or electronic lithography, nanoimprint) enabling to implement spatially resolved patterns of different inorganic materials on a substrate and bottom-up formation of organolayers by spontaneous assembly of molecules on each material. Each inorganic pattern made of a given material exhibits a specific affinity for one or several molecules bearing particular chemical moieties. If the chosen molecules are truly selective of each chosen material, it becomes possible to modify the surface chemical characteristics of each type of pattern.[10] Various combinations of chemical compounds (thiols, silanes, phosphonic acids) and inorganic substrates (Au, SiO_2, metal oxides) have been reported for site selective chemical functionalization using orthogonal surface reactions. For instance, Au/SiO_2 patterned substrates are the most common used template, and selective attachment of thiols to Au and silanes to SiO_2 is exploited.[11–16] Au/metal oxides (TiO_2, Al_2O_3) substrates functionalized with thiols and phosphonic acids have also been achieved thanks to the selective

attachment of the phosphonic acids to metal oxides.[17,18] To our knowledge, orthogonal functionalizations were only explored for surfaces bearing two different materials. However, being able to specifically functionalize surfaces made of more than two materials would provide additional degrees of freedom, and more diversity for new bottom-up nanofabrication approaches.

Herein we have focused on the orthogonal functionalization of Au/SiO_2/TiW substrates. These materials were chosen because they are well established materials in the fields of biosensing (LSPR, QCM…) and/or electronics. In particular, TiW used as a diffusion barrier material has already been reported in electronic devices.[19–25] It is fully compatible with microelectronic integration and could be used as a potential functional membrane in nanoelectronic transducer. TiW thin films can be implemented on a production line with stable and reproducible chemical characteristics. TiW is therefore a material to be considered for implementing complex heterogeneous systems such as nanoelectronic sensors.

In our previous studies, we showed that TiW covered with a native oxide layer could be modified with a phosphonic acid.[26] We also demonstrated that Au/TiW substrate could be orthogonally modified using thiols and phosphonic acids.[27] However with Au/SiO_2/TiW, a challenge arises from the fact that there may be a cross reactivity between SiO_2 and TiW with silane or phosphonic acid.

In this work, we report for the first time in which conditions three-material patterned substrates can be orthogonally functionalized with three different molecules. Au/SiO_2/TiW patterned surfaces were respectively functionalized with thiol, monovalent silane and phosphonic acid. Selectivities of the reactions were assessed by X-ray photoelectron spectroscopy (XPS), infrared spectroscopy (IR), time-of-flight secondary ion mass spectrometry (ToF-SIMS) and

contact angle on three-material substrates bearing either macroscopic features (1 cm) or microscopic features (100 μm) of each material.

EXPERIMENTAL SECTION

Chemicals. 1H,1H,2H,2H-Perfluorodecanethiol (F-thiol) 97% was purchased from Sigma-Aldrich. (Heptadecafluoro-1,1,2,2-tetrahydrodecyl)dimethylchlorosilane (F-silane) 95% was purchased from Abcr. (1H,1H,2H,2H-Tridecafluorooct-1-yl)phosphonic acid (F-phosphonic acid) 95%was purchased from SiKÉMIA. Dichloromethane (DCM) 99.9% was purchased from Sigma-Aldrich then degassed and dried over molecular sieves. Isopropanol 99.9% was purchased from Sigma Aldrich. The ultrapure water (18.2 MΩ) was used for all the experiments and cleaning. It was produced by a Veolia water system.

Patterned surfaces preparing. 3cm x 2cm Au/SiO_2/TiW substrates S1, S2 and S3 were patterned with centimetric size patterns ("macroscale patterned substrates") using the following protocol: one third of each TiW substrate (3 cm x 1 cm) was covered with Ti (5 nm thick) and Au (45 nm thick) by electron beam evaporation (Leybold, 1.5×10^{-6} Torr, 6 kV, 2 Å/s). Another third of each substrate was covered with 50 nm thick SiO_2 film by magnetron sputtering (AC450, Ar 42.7 sccm, O_2 7.5 sccm, RF power 70 W, V_{bias} 140 V, pressure 5×10^{-3} mbar). During Au evaporation and SiO_2 sputtering, a Teflon® tape was used as a masking layer to protect the other two-thirds of the substrate. The remaining third of each substrate remained unchanged as uncovered TiW. A sketch of macroscale patterned substrates is shown in Figure S1. 1cm x 1cm Au/SiO_2/TiW substrates S4, S5, S6 were patterned with ~100 μm characteristic size patterns ("microscale patterned substrates") using a two-steps UV lithography process. AZ 5214 resist was spin coated at 5500 rpm for 30 s, baked at 110 °C for 60 s and exposed through a mask to UV for 4 s using an MBJB4 DUV SUSS Micro Tec device. Development was

performed by immersion of the samples in TMAH (Metal Ion free 726) for 60 s. SiO_2 (50 nm thick) was deposited by magnetron sputtering (AC450, Ar 42.7 sccm, O_2 7.5 sccm, RF power 70 W, V_{bias} 140 V, pressure 5×10^{-3} mbar). Ti (5 nm thick) and Au (45 nm thick) were deposited by electron beam evaporation (Leybold, 1.5×10^{-6} Torr, 6 kV, 2 Å/s). After lift-off, the samples were cleaned by oxygen plasma treatment (Harrick) at the oxygen flow rate of 14 mL/min, RF power level of 38 W for 5 min to ensure that no residual resist remained on the surface. UV lithography process scheme and patterned substrates sketch are shown in Figure S1.

Chemical functionalization. Patterned substrates, named hereafter S1 and S4, were functionalized by F-thiol using the following protocol: substrates were immersed in 25 mL dried DCM containing 100 µL F-thiol (14 mM) for 48 hours. Samples were then rinsed with DCM for 5 min under ultrasound (Branson, 42 kHz, and 100 W) followed by a stream of ultrapure water and dried with nitrogen flow.

Patterned substrates, named hereafter S2 and S5, were functionalized by F-phosphonic acid using the following protocol: substrates were immersed in 20 mL ultrapure water containing 8.5 mg F-phosphonic acid (1 mM) for 16 hours. Substrates were then rinsed with isopropanol for 5 min under ultrasound (Branson, 42 kHz, and 100 W) followed by a stream of ultrapure water and dried with nitrogen flow.

Patterned substrates, named hereafter S3 and S6, were functionalized by F-silane using the following protocol: substrate was immersed in 25 mL dried DCM containing 10 µL F-silane (1 mM) for 48 hours. Then the substrates were rinsed with DCM for 5 min under ultrasound (Branson, 42 kHz, and 100 W) followed by a stream of ultrapure water and dried with nitrogen flow. After F-silane grafting, substrates were immersed in 70 °C ultrapure water for 15 min. After removing the samples were rinsed in ultrapure water and dried with nitrogen flow.

Characterization. X-ray photoelectron spectroscopy (XPS) measurements on macropatterned substrates S1, S2 and S3 were performed using a focused monochromatized X-ray source (Al Kα = 1486.6 eV). Spectrum acquisitions were performed under ultrahigh vacuum conditions (UHV, 10^{-9} Torr). Take-off angle was 90° relative to the substrate surface. Pass energies were 100 eV and 20 eV for wide-scan and high-resolution elemental scans, respectively. Data reduction was performed with CasaXPS software. The dimensions of TiW, SiO_2 and Au macropatterns were largely higher than XPS beam, so that each material of the same substrate could be characterized individually. For each substrate, at least three measurements were performed on different locations of the same material, thus providing triplicate quantitative data for TiW, SiO_2 and Au of the same substrate.

Time-of-flight secondary ion mass spectrometry (ToF-SIMS) measurements were performed on micropatterned substrates S4, S5, S6 with a Physical Electronics TRIFT III instrument (Physical Electronics, Chanhassen, MN) operated with a pulsed Au ion gun (ion current of 2 nA) over a 500 μm × 500 μm area. The ion dose was kept below the static conditions limits. Data were analyzed using WinCadence software. Mass calibration was performed on hydrocarbon secondary ions. For each substrate, at least three measurements were performed on different locations, thus providing triplicate data and images.

Contact angle measurements were performed on macroscopic substrates S1, S2, S3 with a contact angle meter (Digidrop Goniometer, GBX, France) using the sessile drop method with deionized water. At least five 0.6 μL deionized water droplets were used. For each material of the same substrate, contact angle values were averaged from five measurements on different areas.

Attenuated total reflectance Fourier transform infrared (ATR-FTIR) adsorption spectra were recorded on macroscopic substrates S1, S2, S3 using a Thermo Nicolet 6700 spectrometer equipped with an MCT detector cooled with liquid nitrogen. All spectra were obtained from averages of 256 scans at a resolution of 4 cm^{-1}. The dimensions of TiW, SiO_2 and Au macropatterns were largely higher than FTIR beam, so that each material of a same substrate could be characterized individually.

RESULTS AND DISCUSSION

General methodology.

As in previous work described elsewhere[12,26,27], perfluorinated molecules were used because fluorine can be distinctively detected with surface analysis techniques such as XPS, FTIR and ToF-SIMS. This enabled to evaluate where each organic molecule used for surface functionalization was significantly located on multi-material substrates. In the present work, each multi-material substrate ($Au/SiO_2/TiW$) was functionalized with only one type of perfluorinated molecule (F-silane, F-thiol or F-phosphonic acid). Surface analysis techniques were used to assess whether the tested molecule was detectable only on the material it was supposed to be anchored to. Functionalization and washing protocols were explored to reach the best possible functionalization selectivity.

Initial surface and impact of plasma treatment.

Prior to chemical functionalization, the $Au/SiO_2/TiW$ substrates were cleaned using an RF O_2 plasma cleaner. In a previous publication,[26] it was observed that, after oxygen plasma cleaning, the main contributions to the XPS W4f (36.1 and 38.2 eV, $W4f_{7/2}$ and $W4f_{5/2}$, respectively) and Ti 2p (458.6 and 464.4 eV, $Ti2p_{3/2}$ and $Ti2p_{1/2}$, respectively) core levels corresponded to W^{6+}

and Ti $^{4+}$ states in oxides. Furthermore, it was observed that the TiW substrate contains more W than Ti. Finally, under our conditions (oxygen flow rate of 14 mL/min, RF power level of 38 W for 5 min), no gold oxide contribution on the Au4f was observed by XPS.

Following plasma cleaning, each type of substrate was exposed to F-thiol, F-silane or F-phosphonic acid, in order to assess the ability of each molecule to specifically react with one single material of the substrate.

XPS measurements on macropatterned substrates S1, S2, S3.

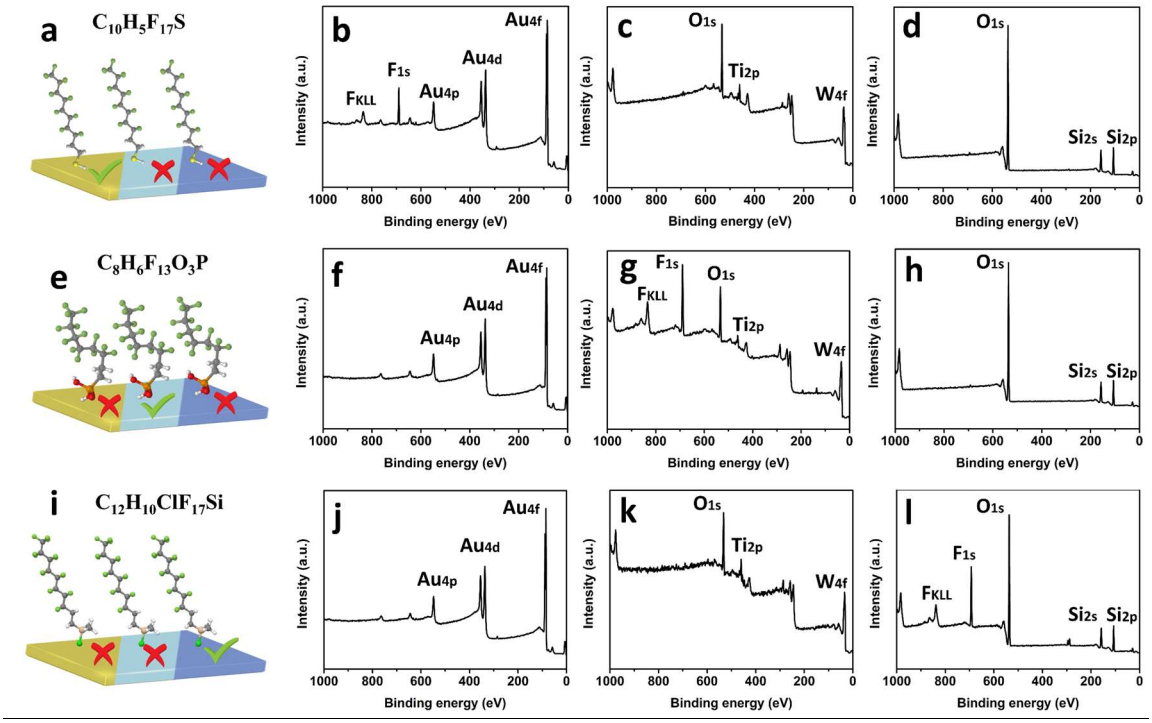

Figure 1. (a) Sketch of macropatterned Au (yellow)/SiO_2 (dark blue)/TiW (light blue) substrate after reaction with F-thiol. On the corresponding XPS survey spectra Au (b), TiW (c) and SiO_2 (d), F 1s and F $_{KLL}$ Auger peaks are only observed on gold suggesting that thiol only bonds to gold. (e) Sketch of macropatterned Au/SiO_2/TiW substrate after reaction with F-phosphonic acid. On the corresponding XPS survey spectra of Au (f), TiW (g) and SiO_2 (h), fluorine XPS peaks were only measured on TiW, suggesting that phosphonic acid only binds to TiW. (i)

Sketch of macropatterned Au/SiO_2/TiW substrate functionalized by F-silane. Fluorine was only present on SiO_2 as suggested by the corresponding XPS survey spectra (Au (j), TiW (k) and SiO_2 (l)).

Organolayers were implemented on macroscale Au/TiW/SiO_2 patterned substrates with respectively F-thiol (Figure 1a), F-silane (Figure 1e) or F-phosphonic acid (Figure 1i) and were analyzed using XPS. Survey and high-resolution spectra were recorded at different areas to probe each material (Au, TiW or SiO_2). Figure 1b-d shows the XPS survey spectra of Au, TiW and SiO_2 areas of macropatterned substrates after incubation with F-thiol. On Au, the presence of fluorine was clearly evidenced by the F 1s and F $_{KLL}$ peaks. On the contrary, fluorine peaks were not observed by XPS on TiW and SiO_2. After incubation of the macroscale patterned substrates with F-phosphonic acid, F 1s and F $_{KLL}$ peaks were only observed on TiW. Such peaks were not observed on Au and SiO_2 (Figure 1f-h). After incubation with F-silane, intense F 1s and F $_{KLL}$ peaks were observed on SiO_2. However, low intensity F 1s peaks were also observed on TiW (Figure S2). Nevertheless, after immersion in 70 °C H_2O for 15 min, the F 1s peak disappeared on TiW, but did not decrease on SiO_2 (Figure 1j-l). Indeed, according to a previous study, the grafting of monovalent silane molecules on TiW is somewhat labile at immersion in 70°C water while TiW bound phosphonic acid remained stable under similar conditions.[26] Therefore, site selective functionalization of SiO_2 on Au/SiO_2/TiW substrate can be achieved providing that the silane molecules can be removed from TiW by hydrolysis of the Si-O-TiW bond. High resolution XPS spectrum of F 1s and C 1s confirmed that the fluorine component observed in each case originated from perfluoromolecules as expected (Figure S3).

Therefore, our XPS results suggested that the orthogonal chemical functionalization of Au/SiO_2/TiW substrate is possible providing that the sample are washed for 15 min at 70 °C in

DI water. To further confirm this orthogonality of the reactions, infra-red spectroscopy, water contact angle and time of flight secondary mass spectrometry were performed.

ATR-FTIR on macropatterned substrates S1, S2, S3.

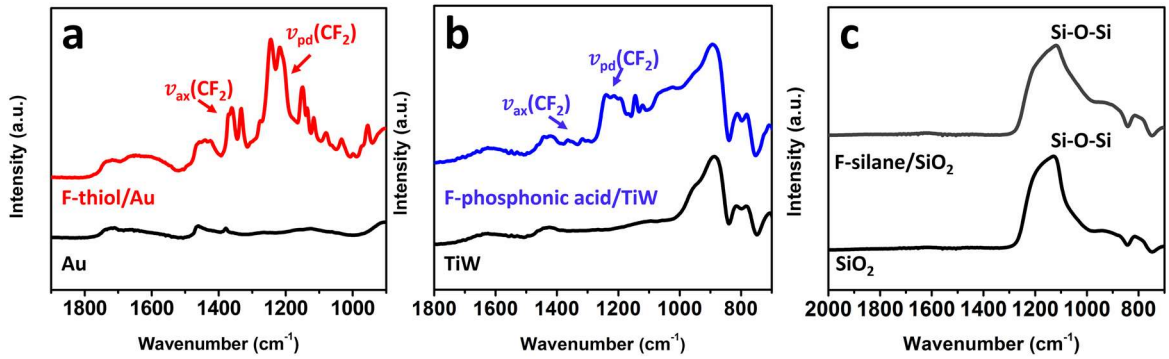

Figure 2. ATR-FTIR spectrum of (a) Au and F-thiol functionalized Au, (b) TiW and F-phosphonic acid functionalized TiW and (c) SiO_2 and F-silane functionalized SiO_2.

ATR-FTIR spectra were recorded on macroscale patterned substrates after incubation with F-thiol, F-phosphonic acid or F-silane. After incubation with F-thiol, the spectra obtained for TiW and SiO_2 areas remained unchanged. However, the spectra corresponding to the Au area displayed clear C-F signatures (Figure 2a). The band at around 1239 cm^{-1} and 1350 cm^{-1} were attributed to the perpendicular CF_2 stretching bands $\upsilon_{pd}CF_2$ and to the axial CF_2 stretching vibration bands $\upsilon_{ax}CF_2$, respectively.[28,29] Similarly, after incubation with F-phosphonic acid, the spectra of Au and SiO_2 remained unchanged. The TiW area displayed clear IR signatures of the symmetric and asymmetric CF_2 vibrations ($\upsilon_{pd}CF_2$ and $\upsilon_{ax}CF_2$) at 1240 cm^{-1} and 1354 cm^{-1}, respectively (Figure 2b). A broad peak from 1080 cm^{-1} to 1100 cm^{-1} was attributed to the P−O bend.[30,31] However, after incubation with F-silane, the spectra of SiO_2 did not have any obvious C−F signatures (Figure 2c). This may be caused by an overlap between the typical CF_2 vibration bands with the Si−O−Si vibration bands.[32]

Water contact angle on macropatterned substrates S1, S2, S3.

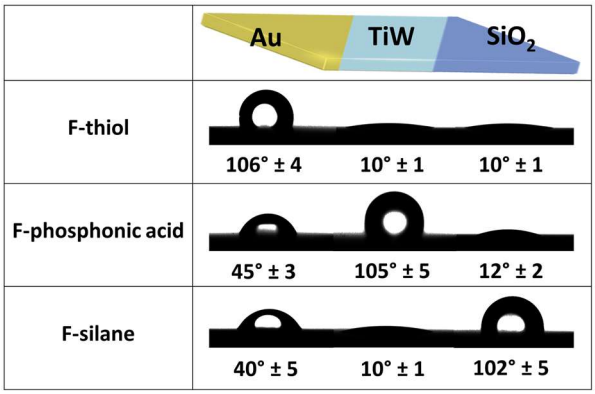

Figure 3. Water contact angles of macropatterned substrates functionalized by F-thiol, F-phosphonic acid, F-silane. (Contact angles of bare Au, TiW and SiO_2 were respective 43°, 12° and 10°)

The typical water contact angles of Au, TiW and SiO_2 regions for the negative controls (patterned substrates immersed in the pure solvent without thiol, silane or phosphonic acid) were 43°, 12° and 10°, respectively. After surface modification with F-thiol, F-phosphonic acid or F-silane, water contact angles were measured for each material of patterned substrates (Figure 3). After incubation of the patterned substrates in the F-thiol solution, the water contact angle of Au area increased to around 105°. The water contact angles of TiW and SiO_2 areas remained similar to the one measured after incubation in the pure solvent suggesting that the surface energy was not affected by the F-thiol. The 105° angle observed on Au was attributed to the formation of a perfluoroalkyl hydrophobic layer on Au.[29] After incubation of the patterned substrates with F-phosphonic acid, the water contact angle on TiW area increased to around 106° due to the formation of hydrophobic F-phosphonic acid layer.[33] Meanwhile, the contact angles of Au and SiO_2 areas remained similar to the original values. Incubation of the patterned substrates with F-silane lead to a water contact angle of 102° on SiO_2, 40° on the TiW areas and 40° on the Au areas. However, after immersion in 70 °C H_2O for 15 min, the

contact angle measured on TiW decreased to nearly 10°. This was attributed to the hydrolysis of the Si-O-M bond.[26]

ToF-SIMS imaging on micropatterned substrates S4, S5, S6.

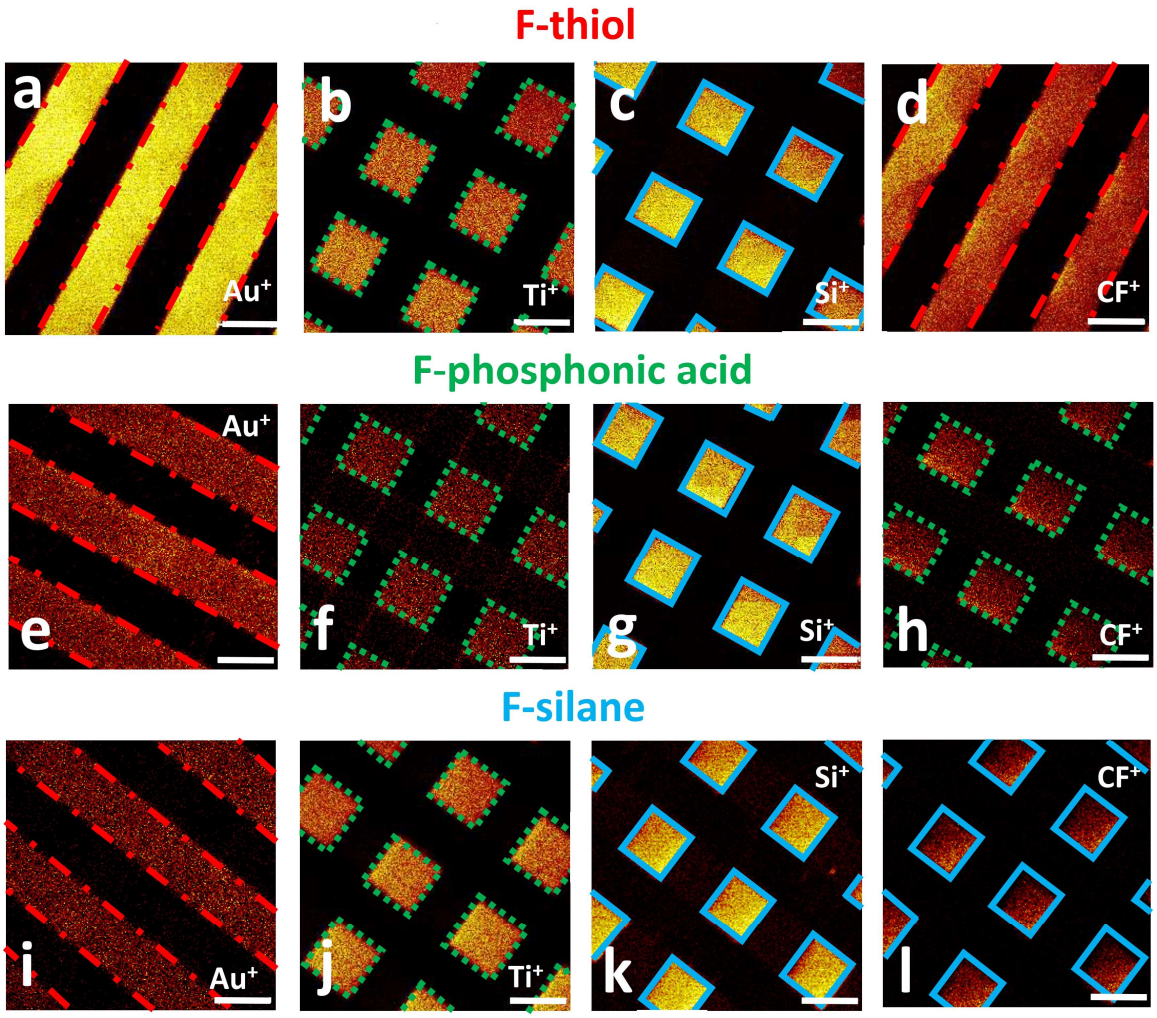

Figure 4. ToF-SIMS imaging of patterned Au/SiO_2/TiW substrates functionalized by F-thiol (a-d), F-phosphonic acid (e-h), or F-silane (i-l). Scale bars =100 µm. After F-silane grafting, the substrates were washed in 70 °C ultrapure water for 15 min. Images a, e, i correspond to the images obtained using Au^+. Similarly, images b, f, j are those obtained with Ti^+, c, g, k with Si^+, and d, h, l with CF^+. Red dot dashed rectangles, green dotted squares and blue solid squares correspond to the Au, TiW and SiO_2 areas, respectively.

Fluorine mapping was performed using ToF-SIMS imaging, which has been shown to be especially well suited for the characterization of chemically patterned surfaces. Au/SiO_2/TiW micropatterned substrates were implemented and imaged by ToF-SIMS after incubation with respectively F-thiol (Figure 4a-d), F-phosphonic acid (Figure 4e-h) or F-silane (Figure 4i-l). For each type of functionalization, all four ions (Au^+, Ti^+, Si^+ and CF^+) signals were imaged and displayed. The Au^+, Ti^+ and Si^+ ions were mainly related to the substrate materials (Au, SiO_2 or TiW) whereas CF^+ ions were related to the chemical functionalization with the fluorinated molecules, respectively F-thiol (a-d), F-phosphonic acid (e-h) or F-silane (i-l) molecule. The substrate related ions Au^+, Ti^+ and Si^+ were observed in all cases allowing for the localization of the information related to the substrate parts. The CF^+ ions were only detected in very specific areas. The orthogonality was assessed by whether the area of CF^+ signal was consistent with area of the three-material ions (Au^+, Ti^+ and Si^+). For example, after incubation with F-thiol (Figure 4a-d), CF^+ (m/z 31.00, Fig.4d, red dot dashed rectangles) and Au^+ (m/z 196.97, red dot dashed rectangles, Fig.4a) originated from the same areas on the same substrate: this suggested that F-thiol is bound to Au zones. On the contrary, areas where Ti^+ (m/z 47.95, Fig.4b, green dotted squares) and Si^+ (m/z 27.98, Fig.4c, blue solid squares) were detected showed no detectable signal of CF^+ ions in Fig4.d: this suggested that F-thiol were only present on Au zones, and not detectable on TiW and SiO2 zones. We therefore interpret that F-thiol was selectively immobilized on Au. Similarly, ToF-SIMS imaging of F-phosphonic acid functionalized substrates (Figure 4e-h) showed that CF^+ (Fig.4h, green dotted squares) was only localized with Ti^+ ions (Fig.4f, green dotted squares), thus suggesting that F-phosphonic acid was only grafted to TiW zones. F-silane functionalized substrates (Figure 4i-l) showed that CF^+ (Fig.4l, blue solid squares) was only colocalized with Si^+ ions (Fig.4k, blue solid squares). This suggested that F-silane was only present on SiO_2.

A challenge addressed in this work was related to the fact that both organosilanes and phosphonic acids were expected to bind metal oxide and silicon dioxide surfaces. However, silanes and phosphonic acids were expected to exhibit different behaviors towards washing and hydrolysis. For instance, Queffélec *et al.* reported that the metal oxide-phosphonic acid bond has a higher robustness and stability than metal-O-Si bonds.[34] Pujari *et al.* mentioned that phosphonic acid layers on metal oxides are particularly stable to hydrolysis by comparison to silane layers, in particular for metals with high oxidation states (+IV tetracoordinate and higher).[35] In the present article we have shown that W is in its +VI oxidation state. Furthermore, we demonstrated in a previous contribution[26] that a monovalent alkoxysilane layer formed on oxidized TiW could be hydrolyzed in 70°C water. These different arguments suggested that a phosphonic acid organolayer on oxidized TiW could be more stable towards aqueous washing than a monosilane organolayer on oxidized TiW. This seems to be confirmed by our experimental results. Besides, Queffélec et al. reported that the stability of a phosphonic acid layer on silicon dioxide was poor, unless a 120-140°C thermal annealing was performed.[34] Thus the selectivity of the silanization reaction for SiO_2 vs TiW on Au/SiO_2/TiW substrate may arise from the stability of the Si-O-Si bond versus the Si-O-Ti or Si-O-W bonds in hot water. The selectivity of phosphonic acid functionalization for oxidized TiW vs SiO_2 may be attributed to the higher stability of phosphonic acid layers on metal oxide by comparison to silicon dioxide.

We did not assess in this work whether monofunctional or trifunctional silanes behave differently towards oxidized TiW or towards SiO_2. We could expect trifunctional silanes such as (tridecafluoro-1,1,2,2-tetrahydrooctyl)trichlorosilane (PFTCS) to behave differently from a monofunctional silane such as heptadecafluoro-1,1,2,2-tetrahydrodecyl)dimethylchlorosilane (PFDCS). For instance, Bright at al.[36] showed that trifunctional perfluorosilane PFTCS could cross-link as a polymeric 3D layer, while monofunctional silane perfluorosilane PFDCS could

form a thin monolayer. This is consistent with a well-known behavior of silanes[37]: trifunctional silanes may 3D cross-link while monofunctional silanes can only bind to the substrate as a (sub)monolayer or make dimers by reacting with another monofunctional silane. Trialkoxysilanes are expected to form 3D cross-linked layers weakly bound to silica through hydrogen bonding, in absence of thermal annealing. However, Tripp et al.[38] and Stewart & Pierce[39] reported that CF_3 moieties can cause an inductive effect on the silicon atom, causing the perfluorinated chlorosilane to be more reactive than a classical chlorosilane without fluorine. Based on such considerations, we could expect fluorinated trichlorosilanes and monochlorosilanes both exhibit a high reactivity towards SiO_2 and oxidized TiW. However, F-trichlorosilanes may be harder to remove from oxidized TiW and SiO_2 than F-monochlorosilanes. Indeed, a cross-linked (or at least laterally linked) silane organolayer would enable multiple anchorage points to surface with possibly lower access to water molecules. Such considerations will need further careful experimental assessments to be correctly explored.

To the best of our knowledge, most of so-far reported orthogonal functionalizations on two-material surfaces involve two steps: functionalization of one material after washing, followed by functionalization of the second material. However, if the functionalizations are truly orthogonal, the functionalizations could be operated simultaneously. Our previous study reported one-pot functionalization procedures of patterned Au on SiO_2 surfaces with thiols and silanes.[12] The next step of this work will consist in performing one-pot functionalization of $Au/SiO_2/TiW$.

CONCLUSIONS

In this paper, we reported on the orthogonal functionalization procedures of patterned Au/SiO_2/TiW substrates with thiols, phosphonic acid and monovalent silane, respectively. The direct chemical characterization using XPS, ATR-FTIR, water contact angle and ToF-SIMS imaging provided evidence of the orthogonality. This orthogonality was obtained, by taking advantage of complementary behaviors: phosphonic acids do not form robust layers on silicon dioxide in the absence of thermal annealing; perfluorinated monochlorosilanes strongly react with SiO_2, possibly because CF_3 enhances reactivity of silane by inductive effect; the selectivity of the silane for silicon dioxide is attributed to the higher stability of the Si-O-Si bond versus the Si-O-Ti or Si-O-W bonds in 70°C water. Similarly, the selectivity of the phosphonic acid for TiW originates from the stability of phosphonic acid layers on high oxidation state metals. TiW surface after O_2 plasma treatment was mainly constituted of WO_3 and TiO_2. In the present work, each perfluorinated molecule was tested individually on substrates composed on three different materials. Two different solvents were used: silane and thiol were used in DCM, while phosphonic acid was used in water. At that stage, our goal was to assess in what conditions each organic molecule could be grafted on only one material among the three materials available on the substrates. The next step will focus on the development of a one pot surface modification of Au/SiO_2/TiW similarly to the protocol reported by Palazon et al[12] with only one single solvent.

Besides, we already had shown how orthogonal functionalizations may be exploited for the deterministic addressing of nanoparticles by electrostatic and bio-affinity methods on two material patterned substrates such as Au/SiO_2 or Au/TiW.[27,40] We expect to perform further localized modification of the surface for the deterministic placement of various nano-object, either anisotropic (e.g. nanoparticles) or isotropic (e.g. nanowires[41]) for various applications including the development of a new generation of sensors and other nanodevices.

ASSOCIATED CONTENT

Supporting Information.

The Supporting Information is available free of charge on the ACS Publications website at DOI:

Two-steps lithography and materials (Au, SiO_2) deposition and lift off process; Optical photos of macropatterned substrates and micropatterned substrates (Figure S1); XPS survey spectra of TiW and SiO_2 regions on macropatterned Au/SiO_2/TiW substrates functionalized by F-silane before immersion in 70 °C ultrapure H_2O (Figure S2); High-resolution XPS C 1s and F 1s spectrum of F-thiol functionalized Au, F-phosphonic acid functionalized TiW and F-silane functionalized SiO_2 (Figure S3) (PDF)

AUTHOR INFORMATION

Corresponding Author

Dr. Yann Chevolot Tel.: +33 (0) 4 72 18 60 58 E-mail: yann.chevolot@ec-lyon.fr

Prof. Jean-Pierre Cloarec Tel.: +33 (0) 4 72 18 62 52 E-mail: jean-pierre.cloarec@ec-lyon.fr

ORCID

Jian Zhang 0000-0002-6358-7158

Yann Chevolot 0000-0003-3479-3371

Jean-Pierre Cloarec 0000-0002-4058-6697

Author Contributions

The manuscript was written through contributions of all authors. All authors have given approval to the final version of the manuscript.

Notes

The authors declare no competing financial interest.

ACKNOWLEDGMENT

J. Z. is grateful to the China Scholarship Council for offering a Ph.D. fellowship. We thank the staff from the NanoLyon platform for their help and technical support.

REFERENCES

(1) Schmidt, R.C.; Healy, K.E. Controlling biological interfaces on the nanometer length scale. *J. Biomed. Mater. Res. A* **2009**, *90*, 1252−1261.

(2) Shi, W.; Xu, T.; Xu, L.P.; Chen, Y.; Wen, Y.; Zhang, X.; Wang, S. Cell micropatterns based on silicone-oil-modified slippery surfaces. *Nanoscale* **2016**, *8*, 18612−18615.

(3) Popova, A.A.; Demir, K.; Hartanto, T.G.; Schmitt, E.; Levkin, P.A. Droplet-microarray on superhydrophobic-superhydrophilic patterns for high-throughput live cell screenings. *Rsc Advances* **2016**, *6*, 38263−38276.

(4) Ruediger, A.; Rosei, F. Interfaces: AFM extends its reach. *Nat. Nanotechnol*. **2010**, *5*, 388−389.

(5) Wilbur, J.L.; Kumar, A.; Biebuyck, H.A.; Kim, E.; Whitesides, G.M. Microcontact printing of self-assembled monolayers: applications in microfabrication. *Nanotechnology* **1996**, *7,* 452−457.

(6) Pan, C.J.; Qin, H.; Nie, Y.D.; Ding, H.Y. Control of osteoblast cells adhesion and spreading by microcontact printing of extracellular matrix protein patterns. *Colloids Surf. B Biointerfaces* **2013**, *104*, 18−26.

(7) Turchanin, A.; Tinazli, A.; El-Desawy, M.; Großmann, H.; Schnietz, M.; Solak, H.H.; Tampe, R.; Gölzhäuser, A. Molecular self-assembly, chemical lithography, and biochemical tweezers: a path for the fabrication of functional nanometer-scale protein arrays. *Adv. Mater*. **2008**, *20*, 471− 477.

(8) Turchanin, A.; Schnietz, M.; El-Desawy, M.; Solak, H.H.; David, C.; Gölzhäuser, A. Fabrication of molecular nanotemplates in self-assembled monolayers by extremeultraviolet-induced chemical lithography. *Small* **2007**, *3*, 2114−2119.

(9) Laibinis, P.E.; Hickman, J.J.; Wrighton, M.S.; Whitesides, G.M. Orthogonal self-assembled monolayers: alkanethiols on gold and alkane carboxylic acids on alumina. *Science* **1989**, *245*, 845− 847.

(10) Gardner, T.J.; Frisbie, C.D.; Wrighton, M.S. Systems for orthogonal self-assembly of electroactive monolayers on Au and ITO: an approach to molecular electronics. *J. Am. Chem. Soc*. **1995**, *117*, 6927−6933.

(11) Bergkvist, M.; Niamsiri, N.; Strickland, A.D.; Batt, C.A. Substrate selective patterning on lithography defined gold on silica: Effect of end-group functionality on intermolecular layer formation. *Surface Science* **2008**, *602*, 2121−2127.

(12) Palazon, F.; Léonard, D.; Le Mogne, T.; Zuttion, F.; Chevalier, C.; Phaner-Goutorbe, M.; Souteyrand, É.; Chevolot, Y.; Cloarec, J.P. Orthogonal chemical functionalization of patterned gold on silica surfaces. *Beilstein J. Nanotechnol*. **2015**, *6*, 2272−2277.

(13) Briand, E.; Humblot, V.; Landoulsi, J.; Petronis, S.; Pradier, C.M.; Kasemo, B.; Svedhem, S. Chemical modifications of Au/SiO_2 template substrates for patterned biofunctional surfaces. *Langmuir* **2010**, *27*, 678−685.

(14) Maeda, K.; Okabayashi, N.; Kano, S.; Takeshita, S.; Tanaka, D.; Sakamoto, M.; Teranishi, T.; Majima, Y. Logic operations of chemically assembled single-electron transistor. *ACS Nano* **2012**, *6*, 2798−2803.

(15) Palma, M.; Abramson, J.J.; Gorodetsky, A.A.; Penzo, E.; Gonzalez Jr, R.L.; Sheetz, M.P.; Nuckolls, C.; Hone, J.; Wind, S.J. Selective biomolecular nanoarrays for parallel singlemolecule investigations. *J. Am. Chem. Soc*. **2011**, *133*, 7656−7659.

(16) Cai, H.; Wind, S.J. Improved glass surface passivation for single-molecule nanoarrays. *Langmuir* **2016**, *32*, 10034−10041.

(17) Burdinski, D.; Saalmink, M.; van den Berg, J.P.; van der Marel, C. Universal ink for microcontact printing. *Angew. Chem., Int. Ed*. **2006**, *45*, 4355−4358.

(18) Feuz, L.; Jönsson, P.; Jonsson, M.P.; Höök, F. Improving the limit of detection of nanoscale sensors by directed binding to high-sensitivity areas. *ACS Nano* **2010**, *4*, 2167−2177.

(19) Wang, C.K.; Chang, S.J.; Su, Y.K.; Chang, C.S.; Chiou, Y.Z.; Kuo, C.H.; Lin, T.K.; Ko, T.K.; Tang, J.J. GaN MSM photodetectors with TiW transparent electrodes. *Mater. Sci. Eng. B* **2004**, *112*, 25−29.

(20) Chiu, H.C.; Chen, C.H.; Yang, C.W.; Kao, H.L.; Huang, F.H.; Peng, S.W.; Lin, H.K. Highly thermally stable in situ SiN_x passivation AlGaN/GaN enhancement-mode high electron mobility transistors using TiW refractory gate structure. *J. Vac. Sci. Technol. B* **2013**, *31*, 051212.

(21) Roshanghias, A.; Khatibi, G.; Pelzer, R.; Steinbrenner, J. On the effects of thickness on adhesion of TiW diffusion barrier coatings in silicon integrated circuits. *Surf. Coat. Technol*. **2014**, *259*, 386−392.

(22) Battegay, F.; Fourel, M. Barrier material selection for TSV last, flipchip & 3D-UBM & RDL integrations. *IEEE Electron. Compon. Technol. Conf.* **2015**, 1183−1192.

(23) Wang, S.; Suthar, S.; Hoeflich, C.; Burrow, B. Diffusion barrier properties of TiW between Si and Cu. *J. Appl. Phys.* **1993**, *73*, 2301−2320.

(24) Chiou, J.C.; Juang, K.C.; Chen, M.C. TiW (N) as diffusion barriers between Cu and Si. *J. Electrochem. Soc*. **1995**, *142*, 2326−2331.

(25) Yan, P.; Li, Y.; Hui, Y.J.; Zhong, S.J.; Zhou, Y.X.; Xu, L.; Liu, N.; Qian, H.; Sun, H.J.; Miao, X.S. Conducting mechanisms of forming-free TiW/Cu_2O/Cu memristive devices. *Appl. Phys. Lett*. **2015**, *107*, 083501.

(26) Zhang, J.; Yeromonahos, C.; Leonard, D.; Géhin, T.; Botella, C.; Grenet, G.; Benamrouche, A.; Penuelas, J.; Monfray, S.; Chevolot, Y.; Cloarec, J.P. Oxidized titanium tungsten surface functionalization by silane, phosphonic acid or ortho-dihydroxyaryl based organolayers. *Langmuir* **2019**, *35*, 9554-9563.

(27) Zhang, J.; Léonard, D.; Mazurczyk, R.; Yeromonahos, C.; Monnier, V.; Géhin, T.; Monfray, S.; Chevolot, Y.; Cloarec, J.P. Orthogonal chemical functionalization of patterned Au/TiW substrate for selective immobilization of nanoparticles. *Nanotechnology* **2019**, *30*, 325601.

(28) Laffineur, F.; Auguste, D.; Plumier, F.; Pirlot, C.; Hevesi, L.; Delhalle, J.; Mekhalif, Z. Comparison between $CH_3(CH_2)_{15}SH$ and $CF_3(CF_2)_3(CH_2)_{11}SH$ monolayers on electrodeposited silver. *Langmuir* **2004**, *20*, 3240−3245.

(29) Patois, T.; Taouil, A.E.; Lallemand, F.; Carpentier, L.; Roizard, X.; Hihn, J.Y.; Bondeau-Patissier, V.; Mekhalif, Z. Microtribological and corrosion behaviors of 1H, 1H, 2H, 2H-

perfluorodecanethiol self-assembled films on copper surfaces. *Surf. Coat. Technol*. **2010**, *205*, 2511−2517.

(30) Daou, T.J.; Begin-Colin, S.; Grenèche, J.M.; Thomas, F.; Derory, A.; Bernhardt, P.; Legaré, P.; Pourroy, G. Phosphate adsorption properties of magnetite-based nanoparticles. *Chem. Mater*. **2007**, *19*, 4494−4505.

(31) Toulemon, D.; Pichon, B.P.; Cattoën, X.; Man, M.W.C.; Begin-Colin, S. 2D assembly of non-interacting magnetic iron oxide nanoparticles via "click" chemistry. *Chem. Commun*. **2011**, *47*, 11954−11956.

(32) Ramin, M.A.; Le Bourdon, G.; Daugey, N.; Bennetau, B.; Vellutini, L.; Buffeteau, T. PMIRRAS investigation of self-assembled monolayers grafted onto SiO_2/Au substrates. *Langmuir* **2011**, *27*, 6076−6084.

(33) McNeill, A.R.; Hyndman, A.R.; Reeves, R.J.; Downard, A.J.; Allen, M.W. Tuning the band bending and controlling the surface reactivity at polar and nonpolar surfaces of ZnO through phosphonic acid binding. *ACS Appl. Mater. Interfaces* **2016**, *8*, 31392−31402.

(34) Queffélec, C.; Petit, M.; Janvier, P.; Knight, D. A.; Bujoli, B. Surface modification using phosphonic acids and esters. *Chem. Rev.* **2012**, *112*, 3777−3807.

(35) Pujari, S. P.; Scheres, L.; Marcelis, A. T. M.; Zuilhof, H. Covalent Surface modification of oxide surfaces. *Angew. Chem. Int. Ed*. **2014**, *53*, 6322−6356.

(36) Bright, L. K., Baker, C. A., Agasid, M. T., Ma, L., & Aspinwall, C. A. Decreased aperture surface energy enhances electrical, mechanical, and temporal stability of suspended lipid membranes. *ACS Appl. Mater. Interfaces* **2013**, 5, 22, 11918–11926.

(37) Fadeev, A. Y., & McCarthy, T. J. Self-assembly is not the only reaction possible between alkyltrichlorosilanes and surfaces: monomolecular and oligomeric covalently attached layers of dichloro-and trichloroalkylsilanes on silicon. *Langmuir* **2000**, 16, 18, 7268–7274.

(38) Tripp, C. P.; Veregin, R. P. N.; Hair, M. L. Effect of fluoroalkyl substituents on the reaction of alkylchlorosilanes with silica surfaces. *Langmuir* **1993**, *9*, 3518–3522.

(39) Steward, O. W.; Pierce, O. R. The effect of substituent fluoroalkyl groups on the alkali-catalyzed hydrolysis of silanes[1]. *J. Am. Chem. Soc.* **1959**, 81, 1983–1985.

(40) Palazon, F.; Rojo-Romeo, P.; Chevalier, C.; Géhin, T.; Belarouci, A.; Cornillon, A.; Zuttion, F.; Phaner-Goutorbe, M.; Souteyrand, E.; Chevolot, Y.; Cloarec, J. P. Nanoparticles selectively immobilized onto large arrays of gold micro and nanostructures through surface chemical functionalizations. *J. Colloid Interface Sci*. **2015**, *447*, 152−158.

(41) Cloarec, J. P., Chevalier, C., Genest, J., Beauvais, J., Chamas, H., Chevolot, Y., Baron, T. & Souifi, A. pH driven addressing of silicon nanowires onto Si_3N_4/SiO_2 micro-patterned surfaces. *Nanotechnology* 2016, 27, 29, 295602.

TOC